IEEE Access
Multidisciplinary | Rapid Review | Open Access Journal

Received 21 April 2023, accepted 13 May 2023, date of publication 23 May 2023, date of current version 1 June 2023.

Digital Object Identifier 10.1109/ACCESS.2023.3279254

RESEARCH ARTICLE

Preventing Over-Enhancement Using Modified ICSO Algorithm

SAHAR AZIMIAN[1], SEYED ALI AMIRSHAHI[2], (Member, IEEE), AND FARAH TORKAMANI AZAR[1]

[1]Faculty of Electrical Engineering, Shahid Beheshti University, Tehran 1983969411, Iran
[2]Colourlab, Norwegian University of Science and Technology, 2815 Gjovik, Norway

Corresponding author: Seyed Ali Amirshahi (s.ali.amirshahi@ntnu.no)

ABSTRACT This paper proposes an Image Contrast Enhancement (ICE) method based on using an Improved Chicken Swarm Optimization (ICSO) algorithm to enhance images while at the same time preventing over-enhancement. In the optimization process, a new practical objective function is employed to reach three main goals, preserving the main details, generating an image with a uniform histogram, and reducing the spikes in the modified histogram. In the proposed approach, the RGB color channels are optimized individually. The performance of the proposed method is suitable for enhancing the contrast of low- and high-contrast images. A subjective experiment is designed to visually evaluate and compare the results with other ICE methods. The simulation results on the CSIQ, TID2013, and SEID datasets show that the proposed method outperforms numerous traditional and state-of-the-art ICE techniques both subjectively and objectively. The most important advantage of the newly proposed technique is that there is an agreement among observers on when over-enhancement occurs regardless of whether the Initial processed image was of low or high contrast.

INDEX TERMS
Contrast enhancement, image quality assessment, over-enhancement.

I. INTRODUCTION

The contrast and brightness of an image are two distinct and objective factors used in image enhancement. Enhancement techniques that focus on contrast can be divided into two different categories, direct and indirect methods [1]. While direct methods define a measure of contrast and find a solution to improve it, indirect methods enhance contrast by increasing or decreasing the dynamic range of pixel values or specific regions in the image without defining a measure of contrast.

Due to its simplicity and efficiency, Histogram Equalization (HE) is a widely used method to enhance image contrast [2]. The image histogram characterizes the number of pixels associated with each intensity value in an image. Simply said, it provides the Probability Distribution Function (PDF) of intensity values in the image. HE operation redistributes intensity values to have a uniform distribution in all brightness values range using the Commutative Density Function (CDF) derived from the PDF of the input image. However, HE mostly results in under- or over-enhancement effects. To address this issue, the Differential gray-level Histogram Equalization (DHE) method was proposed [3]. This approach separated the histogram recursively into sub-histograms depending on local minima and then equalized each sub-histogram within a specific range. DHE avoids checkerboard and washed-out effects and maintains the original mean brightness. The DHE method was later extended to Color Images (DHECI) [4]. The Brightness Preserving Dynamic Histogram Equalization (BPDHE) method was also proposed as an extension of DHE [5] which first applies a Gaussian smoothing to the input histogram and then separates and equalizes sub-histograms and so can enhance images better than DHE. As a modification of BPDHE, Brightness Preserving Dynamic Fuzzy Histogram Equalization (BPFDHE) applied the fuzzy histogram calculation

The associate editor coordinating the review of this manuscript and approving it for publication was Marco Giannelli.

instead of Gaussian filter for smoothing input histograms. In terms of reducing computational time and improving brightness preservation, BPDFHE is a superior method to BPDHE.

A joint HE-based method has recently been presented to improve image contrast using information from the neighboring pixels of each pixel [6]. Despite being simple and taking less time to execute, this method is insufficient to enhance images that have been extremely distorted with regard to their contrast. The Adaptive Contrast Enhancement using Compensated Histogram system (ACECH) is presented based on compensated HE on red, green, and blue channels separately [7]. In terms of enhancing images with slightly low contrast, ACECH is satisfactory, but it fails in terms of enhancing different distortion levels of contrast in images. Fuzzified Contrast Enhancement for Nearly Invisible Images (FCENII) is developed to improve perceptually invisible images [8]. Although FCENII is successful at enhancing invisible images while preserving color information, it does not provide enough enhancement of image details. In other research, Naturalness Balance Contrast Enhancement (NBCE) is introduced to improve image contrast using adaptive gamma with cumulative histogram and median filtering [9]. NBCE retains details successfully, but cannot remove the hazy layer in extremely low contrast images, and its enhanced images look under-enhanced.

Other researchers introduced methods which are based on the clipping of histograms. Among these methods, the Exposure based Sub-Image Histogram Equalization (ESIHE) method was developed for the enhancement of images with low exposure where the image exposure threshold is used for subdividing the image [10]. ESIHE used the maximizing entropy while controlling the enhancement rate making it a better approach for image enhancement. This is particularly the case when it comes to improving underexposed images. As a recursive extension of ESIHE, two versions were proposed [11] which are applied iteratively on an image to reduce the difference in exposure values between successive iterations lower than a particular threshold value. The Dominant Orientation-based Texture Histogram Equalization (DOTHE) was also proposed to overcome the limitations in HE methods [12]. By combining linear channel stretching with histogram averaging, the AVeraging Histogram EQualization approach (AVHEQ) was developed where one-to-one mappings of the intensity levels are performed [13]. This approach yields desirable contrast-enhanced images in terms of brightness conservation, improved global contrast, gradient sharpness of the object, and information content. In [14] and [15] the input histogram is divided adaptively into two or three sub-histograms, and subsequently, each sub-histogram is clipped and modified using a redistribution parameter, and finally, each modified sub-histogram is equalized individually. Such and approach (adaptive division) was also applied in the case of infrared image enhancement [16].

To address such issues in different HE algorithms, optimization problems were also formulated to show the non-linear behavior. The mentioned complex optimization problems can be effectively solved by Nature-Inspired Optimization Algorithms (NIOAs) using single or multiple objective functions [17] and different learning methods. NIOAs such as Artificial Bee Colony (ABC) [18], [19], Cuckoo Search (CS) [20], [21], Particle Swarm Optimization (PSO) [22], Firefly Algorithm (FA) [23], Wind-Driven Optimization (WDO) [24], Chicken Swarm Optimization (CSO) [25], and Moth Swarm Algorithm [26], [27] are effectively used in image processing. NIOAs have been also employed in variant applications such as image segmentation, classification, and compression [28], [29], [30].

In this paper, we focus on the Improved version of CSO optimization algorithm which we refer to as ICSO [31]. In ICSO, to prevent over-enhancement, we introduce special object functions with the aim of improving low- and high-contrast images. CSO is used to solve low-dimensional optimization problems. When it comes to optimizing high-dimensional cases there is a good chance that it will encounter a fall in the local optimum. To overcome this drawback, the improved version (ICSO) is used in our proposed approach. In this paper, our objectives are three-folds:

- First, we introduce a new image enhancement technique using the ICSO algorithm without any over-enhancement or under-enhancement in the image.
- Next, we present a new subjective dataset which includes the subjective evaluation of 21 different observers on 600 images, which are the result of applying the proposed and nine other state-of-the-art image enhancement techniques on 60 different images with high and low contrast.
- Finally, after comparing the results of the objective and subjective evaluations, we investigate the performance of the existing objective Image Quality Metrics (IQMs) on enhanced images.

This paper is structured as follows: Section II introduces advanced brightness and contrast enhancement techniques using ICSO. We introduce the new image dataset and analyze the subjective scores in Section III. Finally, a conclusion of the work is provided in Section IV.

II. PROPOSED APPROACH

Although conventional HE and its variants have been widely used to enhance images whose quality has been affected, by contrast, such methods mostly result in over-enhancement. In this work, we propose a new method (Figure 1) based on an optimization algorithm of CSO and its improved from by defining new object functions which will be able to address over- and under-enhanced images which would also improve image brightness and contrast.

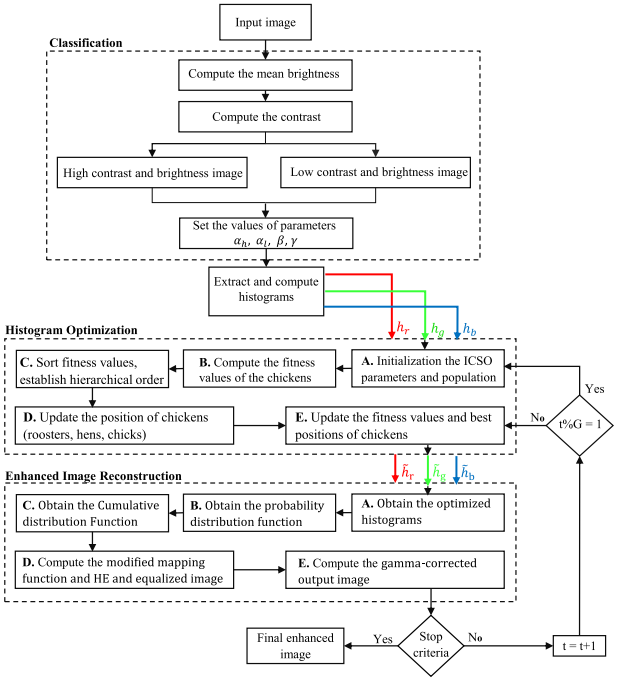

FIGURE 1. The flowchart of the proposed method.

A. CLASSIFICATION OF THE INPUT IMAGE

Although a wide range of image enhancement methods focused on image contrast have been introduced, they are mainly focused on low contrast images or proposed to improve the quality of one type of degraded image [32]. In this study, we aim to introduce a new method to enhance the quality of both low- and high-contrast images. To achieve this goal, we first classify the images into two classes and set the enhancement control parameters based on this classification. This is done by calculating L_m which is the average pixel values in the grayscale ($I_g(x, y)$) version of the color input image ($I(x, y)$). An image with low average pixel values ($L_m \leq 100$) is assumed to be underexposed, while an image with high average pixel values ($150 \leq L_m$) is considered overexposed. The contrast of the image is then calculated by

$$C_{in} = \frac{L_{max} - L_m}{L_{max}}. \tag{1}$$

In eq. (1), L_{max} corresponds to the maximum intensity in I_g. Typically, underexposed images show a low contrast ($C_{in} < 0.5$), while overexposed images show a high contrast ($0.5 < C_{in}$). The details of each step are explained in the following.

B. HISTOGRAM OPTIMIZATION FRAMEWORK USING ICSO

The proposed approach is based on enhancing each color channel in the RGB color space separately. By focusing on the contrast and brightness of the image, the following steps in the ICSO algorithm was used on the histogram ($\mathbf{h}(n)$) in each color channel to preserve the details in the image (Figure 1).

1) INITIALIZATION

The initialization process starts with setting the values of the optimization parameters as the total number of chickens that correspond to the total number of initial states ($N = 150$). This value would then be divided into the three different categories, roosters ($RN = 23$), hens ($HN = 105$), and chicks ($CN = 22$) resulting in a total number of 150. In the case of the hens, we also have a subcategory called mother hens ($MN = 53$) (where $MN \subset HN$). The minimum number of optimization iterations to update the categories elements ($G = 10$), the minimum number of optimization iterations ($Min = 50$) to guarantee receiving a stable state, the maximum number of optimization iterations ($Max = 1000$), and the dimensions of the problem ($D = 256$) that is related to the maximum number of brightness values in the image were specified. In the case of G, a high value would slow down the algorithm in its path to reach the global optimum, while a low value could result in the algorithm reaching the local optimum. This makes selecting the initial value assigned to G a critical matter in the accuracy of the optimization algorithm. The initialization process is then continued by population initialization. In fact, in the ICSO algorithm, N random histograms should be provided to be modified in consecutive iterations to reach the optimum state and then select the best one. To speed up the process, we create N random histograms using the following formula:

$$\begin{aligned} &\tilde{h}_{i,j}(t) = lb + (ub - lb) \cdot rand \cdot h_{i,j}; \\ &for \quad i = 1, \ldots, N, \quad j = 1, \ldots, D \end{aligned} \tag{2}$$

In eq. (2), lb and ub correspond to the minimum and maximum intensity values (here 0 and 255), $rand \in [0, 1]$ is a uniform random number. Therefore, $\tilde{h}_{i,j}(t)$ would be an initialized histogram for the ICSO optimization algorithm. To speed up the optimization procedure, we use the original input histogram for the initial position calculation of 75 chickens ($i \leq 75$). For the rest of them, the equalized input histogram is used ($76 \leq i \leq 150$). The proposed approach in the initial position of the chickens results in fewer optimization iterations.

2) OBJECT FUNCTION

In the next step, the histograms [33] should be selected ordered and based on an objective function. We define a comprehensive objective function

$$\begin{aligned} f_i(t) = &\left\| \tilde{\mathbf{h}}_i(t) - \mathbf{h_i(t)}_2^2 \right\| + \alpha_r \left\| \mathbf{u} - \tilde{\mathbf{h}}_i(t) \right\|_2^2 \\ &+ \|Q_i\|_2^2 + \beta \left\| \mathbf{D} \left[\tilde{\mathbf{h}}_i(t) \right\| = \right]_2^2, \end{aligned} \tag{3}$$

to satisfy our goal (perform image enhancement while at the same time avoid over-enhancement). Initially, to preserve the main details of the input image, it is necessary that the modified histogram ($\tilde{\mathbf{h}}_i(t)$) should be close to the original input histogram ($\mathbf{h_i(t)}$). Since conventional HE methods focus on generating an image with a uniform histogram to maximize the utilization of the dynamic range, the desired histogram

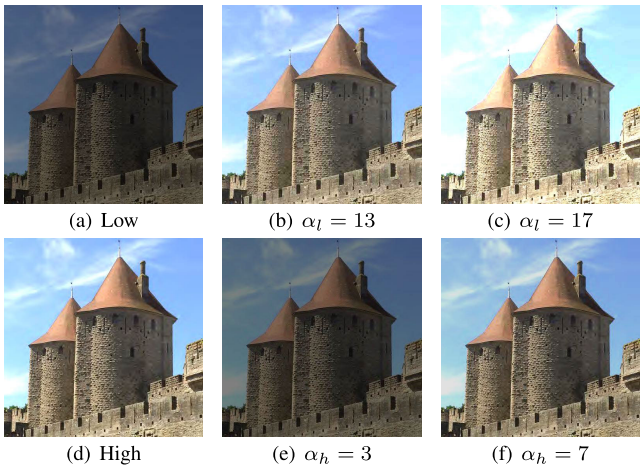

(a) Low (b) $\alpha_l = 13$ (c) $\alpha_l = 17$

(d) High (e) $\alpha_h = 3$ (f) $\alpha_h = 7$

FIGURE 2. Enhanced versions of an image with low and high contrast with different values of α_l and α_h.

needs to be modified as much as possible to reduce residual $\mathbf{u} - \tilde{\mathbf{h}}_i(t)$ which $\mathbf{u}$ is a vector in size histogram with uniform distribution. Moreover, it would be better to determine how close each of the initial histograms are to the uniform histogram ($Q_i = \mathbf{u} - \mathbf{h_i(t)}$). Finally, using an additional penalty term to measure smoothness can help reduce the spikes in the modified histogram. The term $\mathbf{D}\left[\tilde{\mathbf{h}}_i(t)\right]$ was used to measure gradients of $\tilde{\mathbf{h}}_i(t)$ using differential operator D. β is a control parameter of the output histogram smoothing that can vary in the range of $[0, +\infty)$. In our experiments $\beta = 10^4$ was chossen to apply a higher minimization pressure on the gradient value to provide a smoother histogram. $\alpha_r; r \in \{l, h\}$ is a control parameter of contrast enhancement for low and high-contrast input images. In the case of low contrast images, the best variation range for α_l was in the range $[11, 20]$. However, in high contrast images, the best variation range for α_h was $[1, 10]$. Figure 2 demonstrate the effect of selecting α in enhancement results in the processing of low and high-contrast images. A increase in the value of α_r results in an increase in the contrast of the image. In the case of the low contrast input image, when $\alpha_l < 10$ is used, the output image will be under-enhanced. The input image is sufficiently enhanced with $\alpha_l = 13$. Finally, due to the use of $17 \leqslant \alpha_l$, the output image is over-enhanced. In the case of the high contrast input image, the modified histogram is under-enhanced when $\alpha_h = 3$ is used. The input image is sufficiently enhanced at $\alpha_h = 7$, and the details are preserved. Eventually, as a result of using $11 \leqslant \alpha_h$, the output image is over-enhanced with a loss of details.

3) ORDERING FITNESS

The values of ordering fitness as fitness values are computed for all N considered histograms. In ICSO, a good fitness corresponds to a minimal one. By ordering fitness values, histograms are classified into three classes RN, HN, and CN (Previously introduced in Section II-B1). So, the best ones are categorized as roosters followed by hens and chickens respectively. In fact, there are RN groups with roosters as their captain, and hens and chickens are divided between them, randomly.

4) UPDATING THE POSITION OF THE CHICKENS

Following the organization of chicken (rooster, hen, or chick) subgroups, the position (or generated histogram bin values) of all chickens should be updated. That is, [31]: the position of the roosters

$$\tilde{h}_{i,j}(t+1) = \tilde{h}_{i,j}(t) \cdot (1 + randn(0, \sigma^2)) \tag{4}$$

where

$$\sigma^2 = \begin{cases} 1, & f_i(t) \leq f_k(t) \\ exp(\frac{f_k(t) - f_i(t)}{|f_i(t)| + \epsilon}), & f_k(t) < f_i(t) \end{cases} \tag{5}$$

and $randn(0, \sigma^2)$ is a Gaussian distribution with a mean of 0 and a standard deviation of σ^2. In eq. (5), ϵ is used to prevent a denominator of zero in case of small values for $|f_i(t)|$, and $k \neq i, k \in [1, N]$ is the index of other roosters that are randomly selected from the group of roosters. From eq. (4), it is clear that in the case that $f_i(t) \leq f_k(t)$ a larger space is available to search for the i^{th} roster compared to the case that $f_i(t) > f_k(t)$. Next, the positions of the hens are calculated by

$$\begin{aligned} \tilde{h}_{i,j}(t+1) = \tilde{h}_{i,j}(t) &+ S_1 \cdot rand \cdot (\tilde{h}_{r_1,j}(t) - \tilde{h}_{i,j}(t)) \\ &+ S_2 \cdot rand \cdot (\tilde{h}_{r_2,j}(t) - \tilde{h}_{i,j}(t)) \end{aligned} \tag{6}$$

where S_1 and S_2

$$\begin{cases} S_1 = exp(\frac{f_i(t) - f_{r1}(t)}{|f_i(t)| + \epsilon}) \\ S_2 = exp(f_{r2}(t) - f_i(t)) \end{cases}. \tag{7}$$

In eq. (6), r_1 is the rooster index that is the groupmate of the i^{th} hen, and r_2 is the chicken index (rooster or hen) which is selected at random ($r_1 \neq r_2$). Finally, the positions of the chicks are

$$\begin{aligned} \tilde{h}_{i,j}(t+1) = w \cdot \tilde{h}_{i,j}(t) &+ FL \cdot (\tilde{h}_{m,j}(t) - \tilde{h}_{i,j}(t)) \\ &+ C \cdot (\tilde{h}_{r,j}(t) - \tilde{h}_{i,j}(t)) \end{aligned} \tag{8}$$

where

$$w(t) = w_{min} \cdot (\frac{w_{max}}{w_{min}})^{1/(1+10 \cdot t/Max)}. \tag{9}$$

In eq. (8) m is the index of the mother hen for the i^{th} chick and $\tilde{h}_{m,j}(t)$ is its corresponding position. The parameter FL ($FL \in [0, 2]$) indicates that the chick will follow its mother for food. The parameter C indicates that the chicks learn from the rooster in the subgroup. In eq. (9), w is the chicks' self-learning coefficient. As the number of iterations increases, the value of w decreases exponentially from 0.9 to 0.4, t is the number of iterations, and w_{min} and w_{max} represent the final and the initial values of the iterations, respectively. As noted

in the introduction, when the dimension of the problems is high, the CSO will fall in a local optimum. This is because in CSO, chicks learn from their mother hen and their positions do not depend on their associated rooster. Naturally, if their mother falls in a local optimum, they will also fall in a local optimum. To solve this problem, the chick's position in ICSO depends on both their mother hen and rooster, and the learning factor C and self-learning coefficient are also introduced in eq. (8).

5) SELECTION OPTIMUM HISTOGRAM

After an update, fitness values are calculated again using eq. (3) and the minimum fitness value and its corresponding histogram are chosen as the optimized histogram in iteration t.

6) RECONSTRUCTION OF THE OUTPUT IMAGE

The histogram of the input image in the different color channels ($\mathbf{h_k(n)}, k = \{r, g, b\}$) and its enhanced histograms ($\tilde{\mathbf{h}}_k(n)$) are the input and output of each optimization iteration, respectively. Suppose the input image at iteration t ($\mathbf{I(x, y, t)}$), contains N_p number of pixels where their intensity values have a range of 0 to L-1. To achieve a mapping function, the conventional HE is applied to each of the three modified (optimized) histograms $\tilde{\mathbf{h}}_k(n)$ as follows:

1) Compute the Probability Density Function (PDF),

$$\mathbf{p(n)} = \frac{\tilde{\mathbf{h}}_k(n)}{N_p}, \quad \text{for } n \in [0, L-1]. \tag{10}$$

from the optimized histograms.

2) Compute the Cumulative distribution Function (CDF),

$$\mathbf{C(n)} = \sum_{n=0}^{L-1} \mathbf{p(n)}. \tag{11}$$

3) Compute the modified transform function

$$\mathbf{T(n)} = \left\lfloor (L-1)\mathbf{C(n)} + 0.5 \right\rfloor \tag{12}$$

that maps the optimized intensity values to the reconstructed image ($\mathbf{F(x, y, t)}$).

The final enhanced output image is achieved by incorporating gamma correction. This is to improve the image detail in dark and bright areas. The gamma-corrected output image of iteration t is provided by

$$\mathbf{I_o(x, y, t)} = \mathbf{F(x, y, t)}^{\gamma}. \tag{13}$$

The values of gamma γ can change within the range of $[0, 2]$. It is suggested in the case of low brightness, gamma varies between $[0, 1]$, whereas, in the case of high brightness, gamma varies between $[1, 2]$. Once the resulting output image has been provided, it is evaluated to determine whether the stop condition has been met. The three-channel red, green, and blue histograms of the two low and high-contrast input images and the resulting output images (after 178 iterations of optimization) are shown in Figure 3.

7) STOPPING CONDITION OF ALGORITHM

After a minimum number of iterations (for example 50), we have moved from a transient state to the steady state. By using the optimized histogram, the new image ($\mathrm{I}_o(x, y, t)$) is reconstructed after each iteration. Naturally, any iterative process would need a stop condition which we will introduce in the following. For one of the stop conditions we use

$$R_g(t) = \frac{\|G(t)\|_2^2}{\|G(t-1)\|_2^2} \tag{14}$$

which corresponds to the image gradient ration. In eq. (14), $\|G(t)\|_2^2$ corresponds to the second norm of gradient for $\mathbf{I_o(x, y, t)}$. We use the changes in $R_g(t)$ as the first stop condition. That is, if the change in $R_g(t)$ is less than one percent in 50 successive iterations the stop condition is activated. The second stop condition is based on the entropy of the image

$$R_e(t) = \frac{E(t)}{E(t-1)}. \tag{15}$$

where $E(t)$ is the entropy of the modified histogram at iteration t. If $R_e(t)$ changes by less than 1 percent in 50 successive iterations, like $R_g(t)$, the second stopping condition is activated. As the final stop condition we also define a high number corresponding to the maximum number of iterations permitted to execute. Figure 4 shows the values of $R_g(t)$ and $R_e(t)$ for the different iterations for the image shown in 3(a). The figure shows that in the initial iterations, the algorithm is in a transient state, and as the process continues, it reaches a stable state (in this case highest possible image quality), thus the output images have no significant changes and so no need for more iterations. In most cases, the slopes of the changes in values $R_g(t)$ and $R_e(t)$ are the same, and both would trigger the stoppage condition.

It is necessary to point out that, in the case that the algorithm does not meet the stopping conditions, if $t + 1$ is divisible by G (minimum number of optimization iterations to update the categories), the next step would be ordering fitness again to classify all chickens or histograms as roosters, hens, and chicks in a new order so that the formula for updating the histograms is also changed based on their categories. In the case where $t + 1$ is not divisible by G, the previous process continues.

It is important to note that the proposed algorithm is based on the image histogram and therefore results in the stretching of the histogram making the use of color spaces other than RGB unsuitable resulting in unconventional colors in the image. In Figure 5, the effect of the algorithm on only the value component of the HSV color space in two images is shown compared to the processing in RGB channels.

III. EXPERIMENTAL RESULTS

Different studies [34] have shown that current image quality metrics are not able to accurately evaluate the quality of contrast enhanced images. This is why in this study

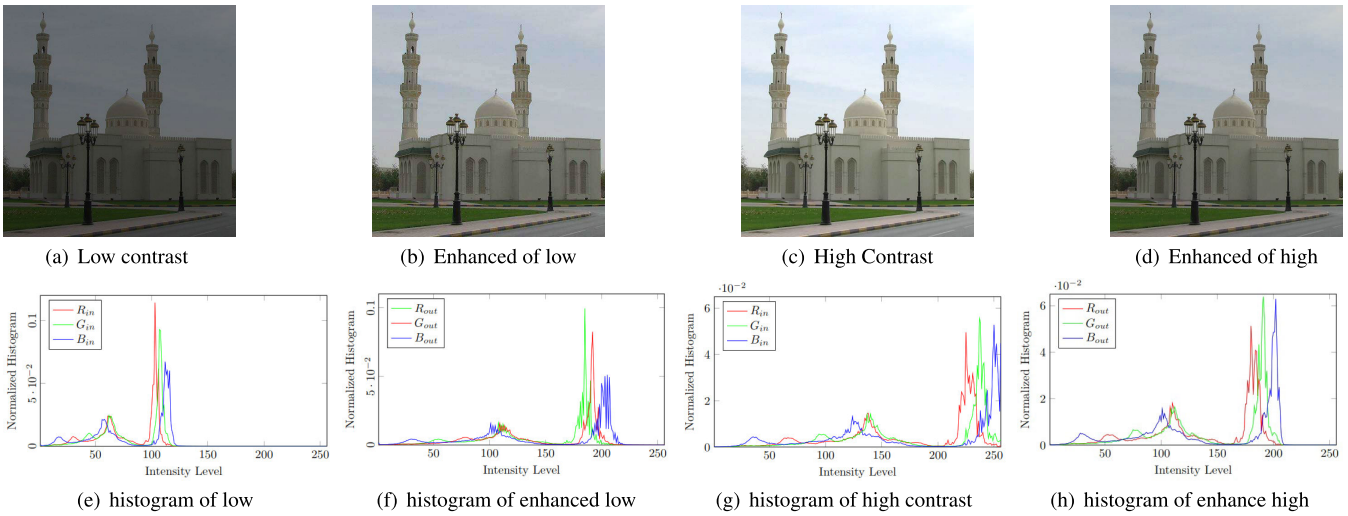

(a) Low contrast (b) Enhanced of low (c) High Contrast (d) Enhanced of high

(e) histogram of low (f) histogram of enhanced low (g) histogram of high contrast (h) histogram of enhance high

FIGURE 3. Input and output images of optimization iterations. (a)-(d) illustrates a low contrast image and a corresponding enhanced image by the proposed method, a high contrast image, and a corresponding enhanced image, respectively. (e)-(h) are corresponding histogram of (a)-(d), respectively.

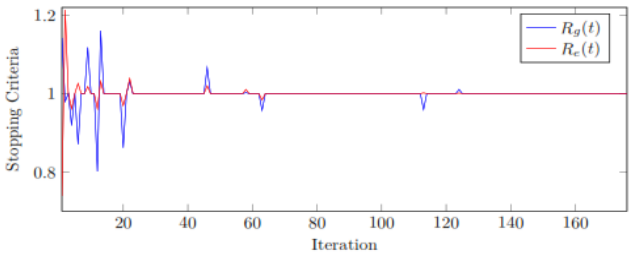

FIGURE 4. $R_g(t)$ and $R_e(t)$ values are illustrated in all iterations at different iterations. The reference image in this case is shown in Figure 3(a) and the enhanced image is shown in Figure 3(b).

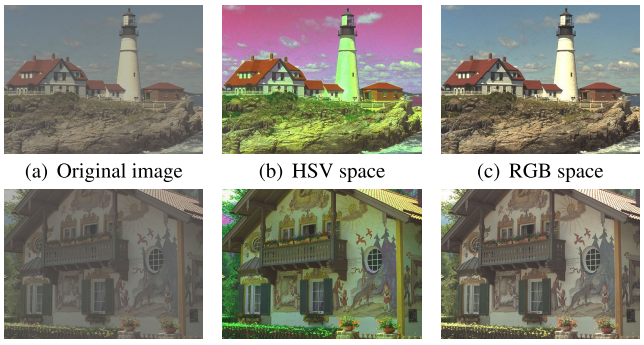

(a) Original image (b) HSV space (c) RGB space

(d) Original image (e) HSV space (f) RGB space

FIGURE 5. The visual results of applying the proposed method on the original image ((a) and (d))using the HSV ((b) and the RGB ((c) and (f)) color space.

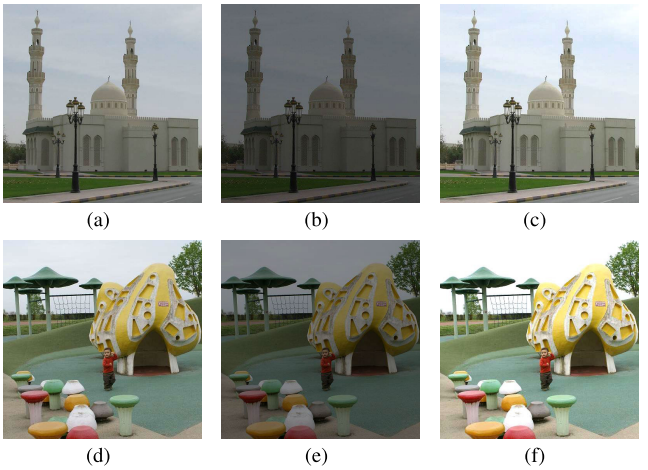

(a) (b) (c)

(d) (e) (f)

FIGURE 6. Two sample images ((a) and (d)) from the SEID dataset [32] along with their corresponding low- ((b) and (e)) and high-contrast ((c) and (f)) test images.

we put a special focus on running a subjective experiment to evaluate the performance of our approach in the cases of low- and high-contrast images. The experiment was tested and performed using MatLab R2020a, which runs on a computer with an Intel Core i7 CPU with 3.4GHz, and Windows 10 (64-bit, 8 GB of RAM) installed as its operating system. We compared the performance of the proposed approach with nine other state-of-the-art methods namely, Adaptive Gamma Correction with Weighting Distribution (AGCWD) [35], Contrast Limited Adaptive Histogram Equalization (CLAHE) [36], Dynamic Piecewise Linear Transformation (DPLT) [37], Exposure based Sub-Image Histogram Equalization (ESIHE) [10], Low-Complexity Algorithm for Contrast Enhancement (LCACE) [38], probabilistic method for image enhancement [39], Automatic and Parameter-Free Piecewise Linear Transformation (APFPLT) [40], image enhancement with Semi-Decoupled Decomposition (SDD) [41], and swift algorithm [42]. The nine methods cover a wide range of different contrast and brightness enhancement techniques which are based on histogram, edges, transforms, mathematical

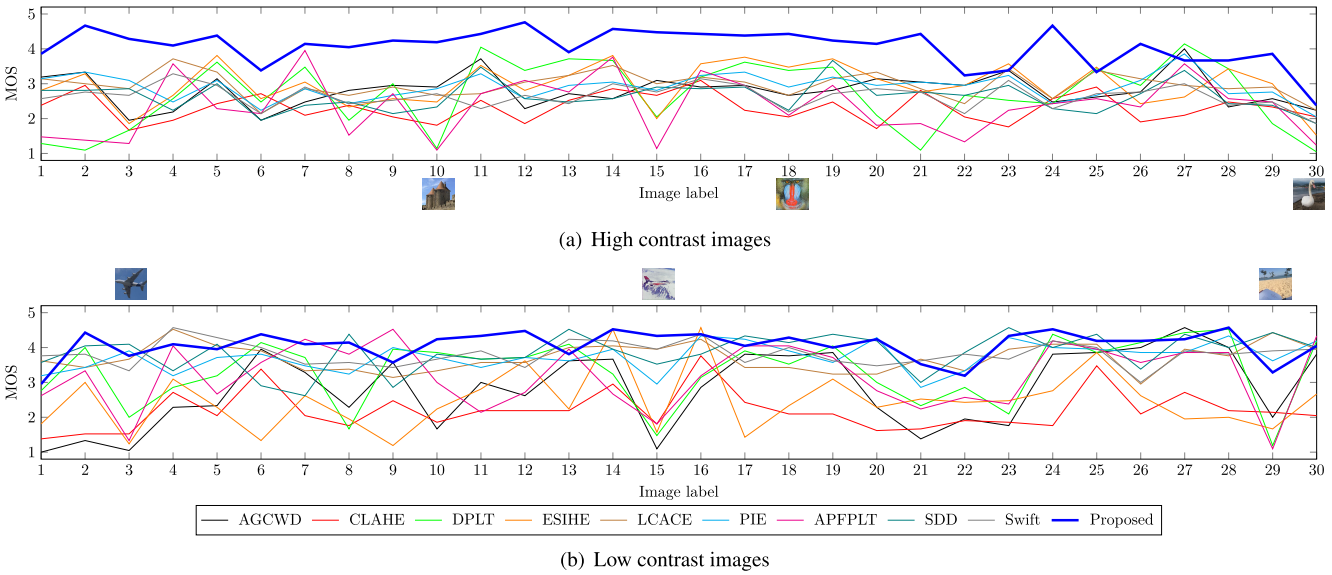

(a) High contrast images

(b) Low contrast images

FIGURE 7. The Distribution of MOS values for each enhancement technique applied on the high- (a) and low-contrast and brightness (b) images. Image labels in the plot correspond to image names in the SEID dataset [32]. Sample images from the dataset are also shown in the plot.

morphology, and HVS-inspired. In our experiment 30 original images from the SEID dataset [32] were selected. The contrast level of these images were then increased and decreased significantly resulting in 60 different (30 low- and 30 high-contrast) images. Sample images from the SEID dataset along with their respective low- and high-contrast images are shown in Figure 6. Such a dataset will enable us to evaluate the performance of different methods in the case of images which are affected by low- and high-contrast distortions. For this the 10 different methods (nine state-of-the-art and our proposed method) were applied to the 60 images resulting in a total of 600 test and 30 reference images. The 600 test images were then shown to the observers in a random order.

21 observers (eight women and 13 men) with an average age of 27.8 (maximum age 60, minimum age 19) participated in our experiment. 15 participants studied or worked in the field of image processing while the others did not have such a background. The Ishihara test was used as a pre-screening tool to exclude observers who were color blind and had poor visual acuity. Observers' vision was normal with a strong or moderate degree of acuity. In the experiments which were collected on the QuickEval platform [43], observers were asked to evaluate the quality of the processed image with respect to the reference image in five categories bad, poor, fair, good, and excellent. To verify the reliability of the observers, 30 images that were selected randomly were repeated. In more than 90% of the cases, the results given by the observers were repeated. Finally, the Mean Opinion Score (MOS) value for each image was used to represent the subjective score for each image. Figures 7(a) and 7(b) show the average MOS for the 60 images in our dataset for the different image enhancement techniques. Results show

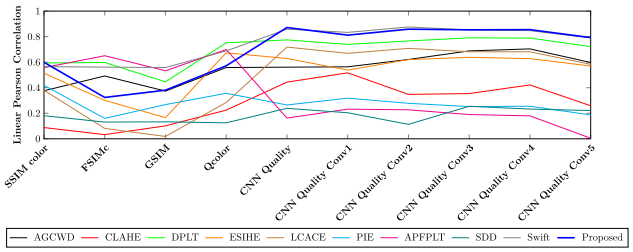

FIGURE 8. Pearson linear correlation coefficient (PLCC) between subjective ratings (MOS) and different state-of-the-art IQMs.

that on average, observers rate the images created through the proposed approach in both high- and low-contrast with a higher score than other image enhancement techniques. It should also be pointed out that in the case of the proposed approach, MOS values tend to show a higher degree of consensus for images with different contents while images enhanced using other techniques show a dramatic change in their quality depending on the image they have been applied on. In addition, most image enhancement techniques perform better in the case of low contrast and bright images. However, the proposed algorithm, works well for images that suffer from high-contrast distortion.

In order to quantitatively evaluate and compare the proposed approach with other methods, different state-of-the-art IQMs were used to evaluate the quality of the output image. These metrics include SSIM color [44], Feature SIMilarity for color images (FSIMc) [45], Gradient SIMilarity (GSIM) [46], Qcolor [47], and the CNN Quality score [48]. Results (Figure 8) show a higher correlation between the subjective and objective scores for the proposed approach compared to other state-of-the-art contrast enhanced metrics.

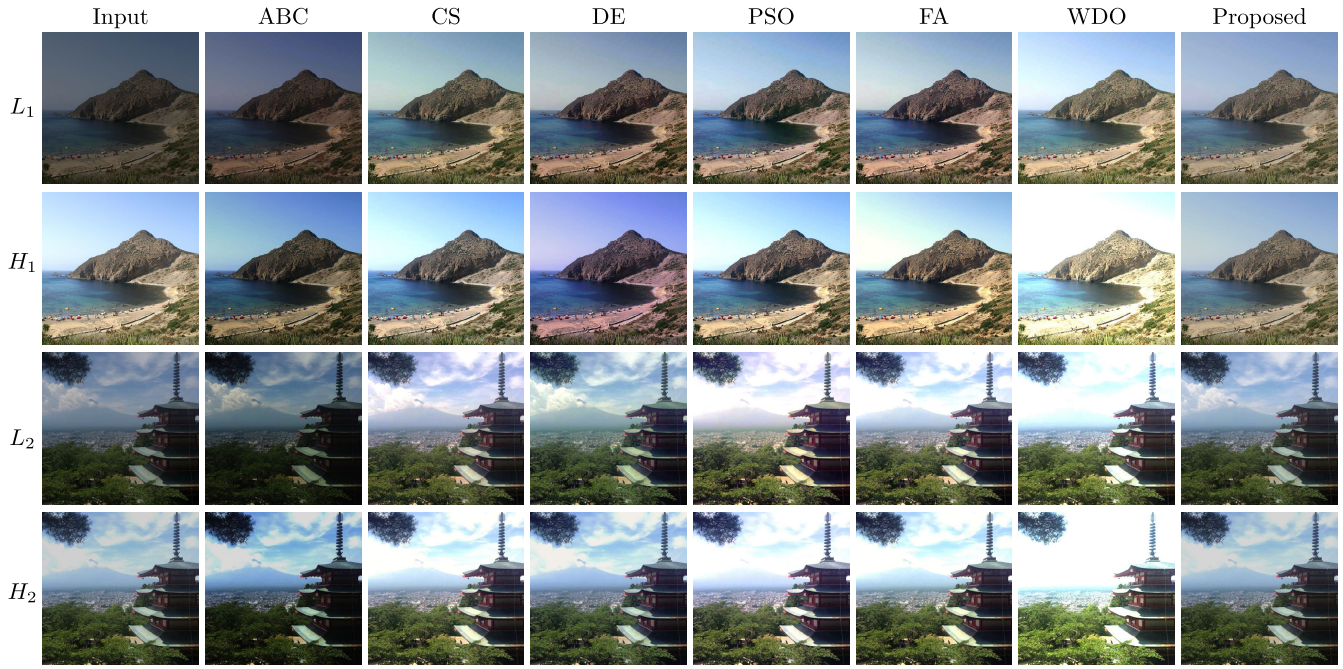

FIGURE 9. Enhanced images using seven optimization-based algorithms on two sample images with low and high contrast with $\alpha_h = 6$, $\alpha_l = 11$, $\gamma = 1$ and $\beta = 10000$ respectively. The enhancement technique used is mentioned above in each column.

TABLE 1. Selection of optimization parameters.

Algorithm	Parameter	Value
ABC [18]	Limit	10
CS [20]	Discovery probability(ρ_a)	0.25
	Step size(α)	1
DE [49]	Crossover constant(CR)	0.2
	Differential weight(F)	0.5
PSO [22]	Cognitive constant($c1$)	3
	Social constant($c2$)	1
FA [23]	Randomness factor(α)	0.5
	Light absorption coefficient(γ)	1
	Attractiveness factor(β)	0.2
WDO [24]	Cravitational acceleration(g)	0.2
	Update equation constant(α)	0.5
	Coriolis effect(c)	0.4
	Maximum allowed speed (V_{max})	0.3

Next, the performance of the proposed method is evaluated using various NIOAs like ABC, CS, DE, PSO, FA, WDO and ICSO. In Table 1, the specific parameters for each NIOA are provided in detail. For all comparisons, the population size is fixed at 150 ($N = 150$).

The results of using seven different optimization-based image enhancement algorithms, including ABC, CS, DE, PSO, FA, WDO, and ICSO (proposed), are compared. The enhanced versions of two pairs of low and high contrast test images from the SEID dataset are shown in Figure 9. For this experiment, α_l, α_h, β, and γ are set 11, 6, 10000, and 1, respectively. In general, in the case of low contrast images, ICSO, CS, and PSO methods provide enhanced images superior to the results of ABC, DE, FA, and WDO methods. Nevertheless, PSO and CS indicate extreme pixel modifications. Consequently, this leads to excessively dark and bright values in the pixel intensities. While in the case of high contrast images, most methods have poor performance, but ICSO, ABC, and DE methods perform significantly greater outcomes than CS, PSO, FA, and WDO methods. Next, in Table 2, the average computation time of the proposed method along with other state-of-the-art methods in seconds is provided. Although the computational time of the proposed approach is relatively longer compared to some other methods, the improvement seen in the quality of the output image would make the use of the proposed approach an attractive option.

In another experiment, severely contrast degraded images belonging to degradation type 17 from the TID2013 dataset [50] (125 images), and 150 images of contrast degradation type from CSIQ dataset [51] were processed by the proposed algorithm and other methods. For visual evaluation, few such images and their output results are shown in Figure 10. As can be seen, in most if not all cases the results of the proposed algorithm are significantly better compared to other approaches. In some cases methods such as DHECI [4], DOTHE [52] and FCENI [8] also show a good performance but this is not consistent among different images in the dataset. In order to quantitatively evaluate the quality of the output images different IQMs were used (Table 3). From the table it is clear that the proposed approach outperforms the other contrast enhancement techniques in both datasets and based on different IQMs.

TABLE 2. Computation time required for each contrast enhancement algorithm in seconds.

CLAHE	DHECI	ESIHE	DOTHE	FCENII	ACECH	NBCE	ABC	CS	DE	PSO	FA	WDO	Proposed
0.146	5.532	0.035	0.363	0.194	0.255	7.06	6.548	2.577	1.851	7.634	8.351	0.946	4.546

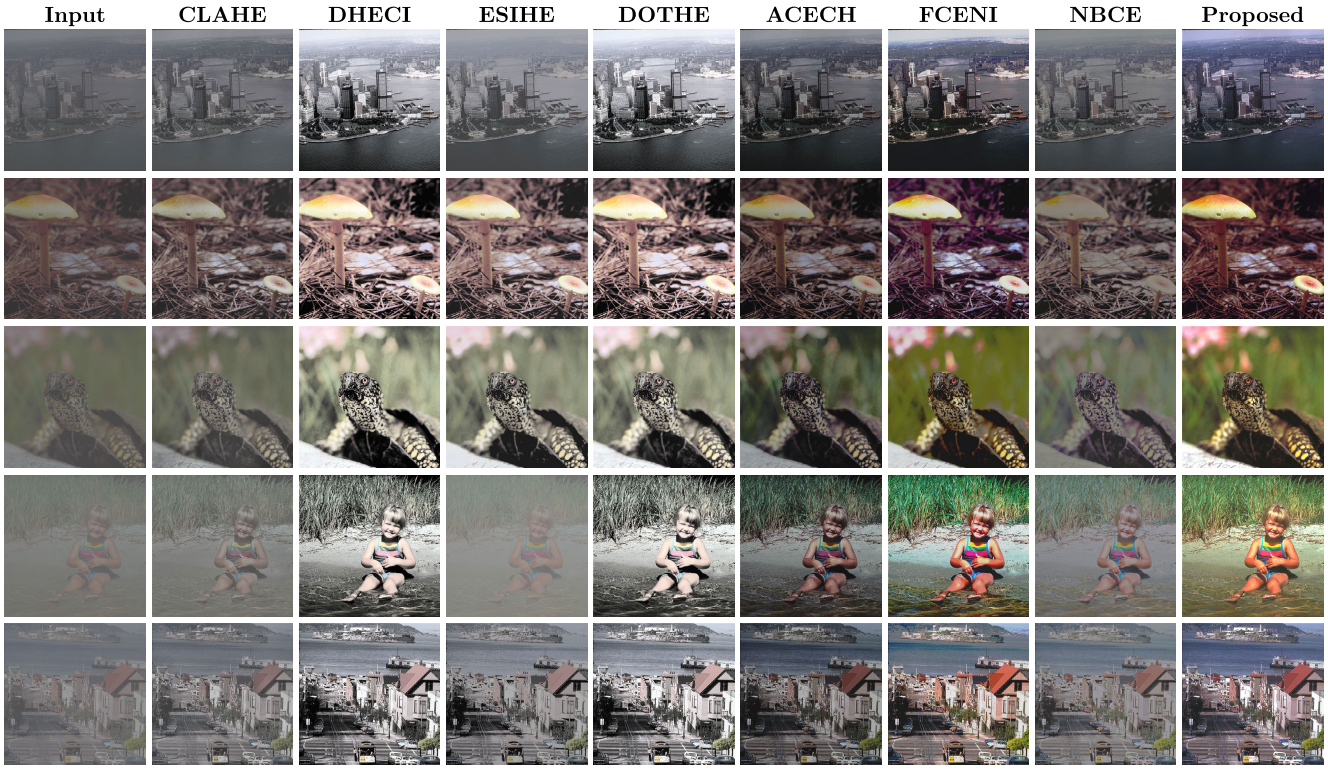

FIGURE 10. Visual comparison of different contrast enhancement techniques compared to the proposed approach. The enhancement technique used is mentioned above each column.

TABLE 3. Mean values of different IQMs calculate for the output image by applying different contrast enhancement techniques on images in the CSIQ and TID2013 dataset which are affected by a contrast related distortion. The best performance for in each IQM is shown in bold characters.

	TID2013 dataset				CIDIQ dataset			
Methods	SSIMcolor	FSIMc	GSIM	Qcolor	SSIMcolor	FSIMc	GSIM	Qcolor
CLAHE	0.911	0.959	0.993	1.436	0.797	0.915	0.985	1.103
DHECI	0.844	0.904	0.982	1.228	0.718	0.910	0.982	0.994
ESIHE	0.901	0.951	0.992	1.371	0.757	0.902	0.983	1.069
DOTHE	0.822	0.890	0.980	1.185	0.792	0.915	0.984	1.124
ACECH	0.869	0.903	0.985	1.337	0.862	0.944	**0.991**	1.226
FCENII	0.815	0.895	0.981	1.002	0.856	0.922	0.988	1.066
NBCE	0.884	0.920	0.989	1.258	0.796	0.900	0.985	1.046
Proposed	**0.980**	**0.989**	**0.998**	**1.560**	**0.902**	**0.951**	**0.991**	**1.335**

IV. CONCLUSION

In this study, we investigated how to enhance the quality of both low and high contrast images while at the same time preventing over-enhancement. For this purpose, we used the improved algorithm of ICSO for optimization.The main contribution of the work is the definition of the terms in the criterion function which allows the preserving of the main details in the input image, similarity of the modified histogram in the input histogram, modifies the output histogram to better correspond to a uniform distribution, and finally measure the smoothness to reduce the spikes in the modified histogram with the goal of preventing over enhancement as well as the definitions of the stopping conditions for the algorithm. As the algorithm reaches a stable state and the gradient and entropy of the output image do not change, the system stops. This method employs three parameters to control brightness and contrast enhancement levels and preserve the main details. Through a subjective experiment and the use of different IQMs, we see a better performance of the proposed approach compared to other techniques.

REFERENCES

[1] A. Beghdadi, M. A. Qureshi, S. A. Amirshahi, A. Chetouani, and M. Pedersen, "A critical analysis on perceptual contrast and its use in visual information analysis and processing," *IEEE Access*, vol. 8, pp. 156929–156953, 2020.

[2] R. Gonzalez and R. Woods, *Digital Image Processing*. Upper Saddle River, NJ, USA: Prentice-Hall, 2002.

[3] M. Abdullah-Al-Wadud, M. H. Kabir, M. A. A. Dewan, and O. Chae, "A dynamic histogram equalization for image contrast enhancement," *IEEE Trans. Consum. Electron.*, vol. 53, no. 2, pp. 593–600, May 2007.

[4] K. Nakai, Y. Hoshi, and A. Taguchi, "Color image contrast enhacement method based on differential intensity/saturation gray-levels histograms," in *Proc. Int. Symp. Intell. Signal Process. Commun. Syst.*, Nov. 2013, pp. 445–449.

[5] H. Ibrahim and N. Pik Kong, "Brightness preserving dynamic histogram equalization for image contrast enhancement," *IEEE Trans. Consum. Electron.*, vol. 53, no. 4, pp. 1752–1758, Nov. 2007.

[6] S. Agrawal, R. Panda, P. K. Mishro, and A. Abraham, "A novel joint histogram equalization based image contrast enhancement," *J. King Saud Univ.-Comput. Inf. Sci.*, vol. 34, no. 4, pp. 1172–1182, Apr. 2022.

[7] A. Kumar, A. K. Bhandari, and R. Kumar, "3D color channel based adaptive contrast enhancement using compensated histogram system," *Multimedia Syst.*, vol. 27, Feb. 2021, Art. no. 563580.

[8] R. Kumar and A. K. Bhandari, "Fuzzified contrast enhancement for nearly invisible images," *IEEE Trans. Circuits Syst. Video Technol.*, vol. 32, no. 5, pp. 2802–2813, May 2022.

[9] P. Singh, A. K. Bhandari, and R. Kumar, "Naturalness balance contrast enhancement using adaptive gamma with cumulative histogram and median filtering," *Optik*, vol. 251, Feb. 2022, Art. no. 168251.

[10] K. Singh and R. Kapoor, "Image enhancement using exposure based sub image histogram equalization," *Pattern Recognit. Lett.*, vol. 36, pp. 10–14, Jan. 2014.

[11] K. Singh, R. Kapoor, and S. K. Sinha, "Enhancement of low exposure images via recursive histogram equalization algorithms," *Optik*, vol. 126, no. 20, pp. 2619–2625, Oct. 2015.

[12] K. Singh, D. K. Vishwakarma, G. S. Walia, and R. Kapoor, "Contrast enhancement via texture region based histogram equalization," *J. Mod. Opt.*, vol. 63, no. 15, pp. 1444–1450, Aug. 2016.

[13] S. C. F. Lin, C. Y. Wong, M. A. Rahman, G. Jiang, S. Liu, N. Kwok, H. Shi, Y.-H. Yu, and T. Wu, "Image enhancement using the averaging histogram equalization (AVHEQ) approach for contrast improvement and brightness preservation," *Comput. Electr. Eng.*, vol. 46, pp. 356–370, Aug. 2015.

[14] A. Paul, P. Bhattacharya, and S. P. Maity, "Histogram modification in adaptive bi-histogram equalization for contrast enhancement on digital images," *Optik*, vol. 259, Jun. 2022, Art. no. 168899.

[15] A. Paul, "Adaptive tri-Plateau limit tri-histogram equalization algorithm for digital image enhancement," *Vis. Comput.*, vol. 39, no. 1, pp. 297–318, Jan. 2023.

[16] A. Paul, T. Sutradhar, P. Bhattacharya, and S. P. Maity, "Infrared images enhancement using fuzzy dissimilarity histogram equalization," *Optik*, vol. 247, Dec. 2021, Art. no. 167887.

[17] K. G. Bdhal, A. Das, S. Ray, J. Gálvez, and S. Das, "Histogram equalization variants as optimization problems: A review," *Arch. Comput. Methods Eng.*, vol. 28, pp. 1471–1496, Apr. 2021.

[18] D. Karaboga and B. Basturk, "A powerful and efficient algorithm for numerical function optimization: Artificial bee colony (ABC) algorithm," *J. Global Optim.*, vol. 39, no. 3, pp. 459–471, Oct. 2007.

[19] J. Chen, W. Yu, J. Tian, L. Chen, and Z. Zhou, "Image contrast enhancement using an artificial bee colony algorithm," *Swarm Evol. Comput.*, vol. 38, pp. 287–294, Feb. 2018.

[20] X.-S. Yang and S. Deb, "Cuckoo search via Lévy flights," in *Proc. World Congr. Nature Biologically Inspired Comput. (NaBIC)*, 2008, pp. 210–214.

[21] L. Maurya, V. Lohchab, P. K. Mahapatra, and J. Abonyi, "Contrast and brightness balance in image enhancement using cuckoo search-optimized image fusion," *J. King Saud Univ.-Comput. Inf. Sci.*, vol. 34, no. 9, pp. 7247–7258, Oct. 2022.

[22] J. Kennedy and R. Eberhart, "Particle swarm optimization," in *Proc. Int. Conf. Neural Netw. (ICNN)*, vol. 4, 1995, pp. 1942–1948.

[23] X.-S. Yang, "Firefly algorithm, Lévy flights and global optimization," in *Research and Development in Intelligent Systems XXVI*. London, U.K.: Springer, 2010, pp. 209–218.

[24] Z. Bayraktar, M. Komurcu, and D. H. Werner, "Wind driven optimization (WDO): A novel nature-inspired optimization algorithm and its application to electromagnetics," in *Proc. IEEE Antennas Propag. Soc. Int. Symp.*, Jul. 2010, pp. 1–4.

[25] X. Meng, Y. Liu, X. Gao, and H. Zhang, "A new bio-inspired algorithm: Chicken swarm optimization," in *Proc. Int. Conf. Swarm Intell.*, vol. 8794. Cham, Switzerland: Springer, 2014, pp. 86–94.

[26] A. Luque-Chang, E. Cuevas, A. Chavarin, and M. Perez, "Agent-based image contrast enhancement algorithm," *IEEE Access*, vol. 11, pp. 6060–6077, 2023.

[27] A. Luque-Chang, E. Cuevas, M. Pérez-Cisneros, F. Fausto, A. Valdivia-González, and R. Sarkar, "Moth swarm algorithm for image contrast enhancement," *Knowl.-Based Syst.*, vol. 212, Jan. 2021, Art. no. 106607.

[28] Q. Luo, J. Li, and Y. Zhou, "Spotted hyena optimizer with lateral inhibition for image matching," *Multimedia Tools Appl.*, vol. 78, Aug. 2019, Art. no. 3427734296.

[29] K. Sivanantham, I. Kalaiarasi, and B. Leena, "Brain tumor classification using hybrid artificial neural network with chicken swarm optimization algorithm in digital image processing application," in *Advance Concepts of Image Processing and Pattern Recognition: Effective Solution for Global Challenges*. Singapore: Springer, 2022, pp. 91–108.

[30] N. Bharanidharan and H. Rajaguru, "Improved chicken swarm optimization to classify dementia MRI images using a novel controlled randomness optimization algorithm," *Int. J. Imag. Syst. Technol.*, vol. 30, no. 3, pp. 605–620, Sep. 2020.

[31] D. Wu, F. Kong, W. Gao, Y. Shen, and Z. Ji, "Improved chicken swarm optimization," in *Proc. IEEE Int. Conf. Cyber Technol. Autom., Control, Intell. Syst. (CYBER)*, Jun. 2015, pp. 681–686.

[32] S. Azimian, F. T. Azar, and S. A. Amirshahi, "How good is too good? A subjective study on over enhancement of images," in *Proc. Color Imag. Conf.*, 2021, pp. 83–88.

[33] T. Arici, S. Dikbas, and Y. Altunbasak, "A histogram modification framework and its application for image contrast enhancement," *IEEE Trans. Image Process.*, vol. 18, no. 9, pp. 1921–1935, Sep. 2009.

[34] S. A. Amirshahi, A. Kadyrova, and M. Pedersen, "How do image quality metrics perform on contrast enhanced images?" in *Proc. 8th Eur. Workshop Vis. Inf. Process. (EUVIP)*, Oct. 2019, pp. 232–237.

[35] S.-C. Huang, F.-C. Cheng, and Y.-S. Chiu, "Efficient contrast enhancement using adaptive gamma correction with weighting distribution," *IEEE Trans. Image Process.*, vol. 22, no. 3, pp. 1032–1041, Mar. 2013.

[36] K. Zuiderveld, *Contrast Limited Adaptive Histogram Equalization*. Amsterdam, The Netherlands: Elsevier, 1994, pp. 474–485.

[37] S. Soc, "Color image enhancement by using dynamic piecewise linear transformation," presented at the Sirindhorn Int. Thai-German Graduate School Eng., King Mongkut's Univ. of Technology North Bangkok, Nov. 27, 2018.

[38] Z. Al-Ameen and Z. A. Hasan, "A low-complexity algorithm for contrast enhancement of digital images," *Int. J. Image, Graph. Signal Process.*, vol. 10, no. 2, pp. 60–67, Feb. 2018.

[39] X. Fu, Y. Liao, D. Zeng, Y. Huang, X. Zhang, and X. Ding, "A probabilistic method for image enhancement with simultaneous illumination and reflectance estimation," *IEEE Trans. Image Process.*, vol. 24, no. 12, pp. 4965–4977, Dec. 2015.

[40] C.-M. Tsai and Z.-M. Yeh, "Contrast enhancement by automatic and parameter-free piecewise linear transformation for color images," *IEEE Trans. Consum. Electron.*, vol. 54, no. 2, pp. 213–219, May 2008.

[41] S. Hao, X. Han, Y. Guo, X. Xu, and M. Wang, "Low-light image enhancement with semi-decoupled decomposition," *IEEE Trans. Multimedia*, vol. 22, no. 12, pp. 3025–3038, Dec. 2020.

[42] Z. Al-Ameen, "Expeditious contrast enhancement for grayscale images using a new swift algorithm," *Statist., Optim. Inf. Comput.*, vol. 6, no. 4, pp. 577–587, Nov. 2018.

[43] K. Van Ngo, J. J. Storvik, C. A. Dokkeberg, I. Farup, and M. Pedersen, "QuickEval: A web application for psychometric scaling experiments," *Proc. SPIE*, vol. 9396, pp. 212–224, Feb. 2015.

[44] N. Bonnier, F. Schmitt, H. Brettel, and S. Berche, "Evaluation of spatial gamut mapping algorithms," in *Proc. Color Imag. Conf.*, 2006, pp. 56–61.

[45] L. Zhang, L. Zhang, X. Mou, and D. Zhang, "FSIM: A feature similarity index for image quality assessment," *IEEE Trans. Image Process.*, vol. 20, no. 8, pp. 2378–2386, Aug. 2011.

[46] A. Liu, W. Lin, and M. Narwaria, "Image quality assessment based on gradient similarity," *IEEE Trans. Image Process.*, vol. 21, no. 4, pp. 1500–1512, Apr. 2012.
[47] Z. Wang and A. C. Bovik, "A universal image quality index," *IEEE Signal Process. Lett.*, vol. 9, no. 3, pp. 81–84, Mar. 2002.
[48] S. A. Amirshahi, M. Pedersen, and X. S. Yu, "Image quality assessment by comparing CNN features between images," *J. Imag. Sci. Technol.*, vol. 60, no. 6, pp. 60410:1–60410:10, 2016.
[49] R. Storn and K. Price, "A simple and efficient heuristic for global optimization over continuous spaces," *Global Optim.*, vol. 11, no. 4, pp. 341–359, 1997.
[50] N. Ponomarenko, L. Jin, O. Ieremeiev, V. Lukin, K. Egiazarian, J. Astola, B. Vozel, K. Chehdi, M. Carli, F. Battisti, and C.-C. Jay Kuo, "Image database TID2013: Peculiarities, results and perspectives," *Signal Process., Image Commun.*, vol. 30, pp. 57–77, Jan. 2015.
[51] D. M. Chandler, "Most apparent distortion: Full-reference image quality assessment and the role of strategy," *J. Electron. Imag.*, vol. 19, no. 1, Jan. 2010, Art. no. 011006.
[52] Y. Wang, Q. Chen, and B. Zhang, "Image enhancement based on equal area dualistic sub-image histogram equalization method," *IEEE Trans. Consum. Electron.*, vol. 45, no. 1, pp. 68–75, Feb. 1999.

SAHAR AZIMIAN received the B.Sc. degree in electrical engineering from the Hamedan University of Technology, Iran, in 2013, and the M.Sc. degree in telecommunication engineering from Shahid Beheshti University, Iran, in 2022. Her research interests include objective and subjective image quality assessment and image enhancement.

SEYED ALI AMIRSHAHI (Member, IEEE) received the B.Sc. degree in electrical engineering from the Amirkabir University of Technology, Iran, in 2008, the Graduate degree from the Master Erasmus Mundus Color in Informatics and Media Technology (CIMET) Program, in 2010, and the Ph.D. degree from the Computer Vision Group, Friedrich Schiller University Jena, Germany, in 2015. In 2016, he was a Postdoctoral Fellow with the International Computer Science Institute (ICSI), Berkeley, CA, USA. From 2017 to 2019, he was a FRIPRO/Marie Sklodowska-Curie Postdoctoral Fellow with the Norwegian University of Science and Technology (NTNU), Gjovik, and a Visiting Researcher with the University of Paris 13 (Institut Galilée) Sorbonne Paris Cite. He is currently an Associate Professor with the Department of Computer Science, NTNU. He is also a member of the Colourlab. His research interest includes image and video quality assessment.

FARAH TORKAMANI AZAR received the B.S. degree in electrical engineering from the Amirkabir University of Technology, Tehran, Iran, in 1986, the M.S. degree in electrical engineering from the Isfahan University of Technology, Isfahan, Iran, in 1991, and the Ph.D. degree from New South Wales University, Sydney, NSW, Australia, in 1995. She was an Academic Staff with the Isfahan University of Technology, from 1995 to 2000. Since 2000, she has been a member of the Communication Department, Shahid Beheshti University, Tehran, where she is currently an Associate Professor. Her current research interests include several aspects of signal processing, specially in image processing, compressive sensing, graph signal processing, and deep learning.